Regular Paper
J. Korean Inst. Electr. Electron. Mater. Eng.
Vol. 30, No. 12, pp. 817-821 December 2017
DOI: https://doi.org/10.4313/JKEM.2017.30.12.817
ISSN 1226-7945(Print), 2288-3258(Online)

Electrical Characteristic Changes of ZnO Varistors by Energy Absorption

Woo-Hyun Kim[1], Seong-Cheol Hwang[1], Guoming Wang[1], Gyung-Suk Kil[1,a], and Chang-Hwan Ahn[2]

[1] Department of Electrical and Electronics Engineering, Korea Maritime and Ocean University, Busan 49112, Korea
[2] Department of Digital Electronics, Inha Technical College, Incheon 22212, Korea

(Received October 13, 2017; Revised October 21, 2017; Accepted October 24, 2017)

Abstract: As a ZnO varistor is subjected to electrical and environmental stresses, it degrades gradually, which may result in power interruption by short circuit. This study investigates changes in the electrical characteristics of ZnO varistors due to deterioration owing to energy absorption, and determines the optimal parameters for on-line diagnosis of the varistor. Two types of varistors were used for an accelerated aging experiment involving the application of the 8/20 μs standard lightning impulse current. The electrical characteristics in terms of the reference voltage, total leakage current, resistive leakage current, and third-harmonic component of the total leakage current were measured, and their change rates were analyzed. The results revealed that the total leakage current increased slightly with an increase in the varistor absorbed energy, while the resistive leakage current and the third-harmonic component increased apparently. Therefore, the third-harmonic component of the total leakage current was proposed as the optimal parameter for on-line monitoring of ZnO varistor conditions.

Keywords: ZnO varistor, Accelerated aging experiment, Deterioration, Energy absorption, Reference voltage, Leakage current, On-line condition monitoring

1. INTRODUCTION

A metal-oxide ZnO varistor equipped in the low-voltage system is used to protect the downstream electronic circuits or devices against the surges and transient overvoltages. As the electronic component and semiconductor device have became more and more important in the system, they should be fully protected to ensure the stable and reliable operation. Therefore, the varistor, which has advantages of high non-linearity, large energy absorption ability, and fast response, has been widely applied. And the performances of varistor are specified in various standards [1-4].

ZnO varistor degrades gradually due to repetitive operations and environmental stresses [5]. As a result, its leakage current increases even at the rated voltage and finally the varistor fails in the form of short circuit, leading to the line-to-ground fault of the equipment. Therefore, the techniques for off-line and on-line condition monitoring of ZnO varistor are necessary to avoid the accident or outage due to the deterioration of varistor. With the progresses of deterioration, the performance of varistor declines and its electrical characteristics, including the reference voltage, total leakage current, resistive leakage current, and harmonic components of total leakage current changes [6-8]. It is specified by the manufactures that the varistor should be replaced onces its reference voltage changes by ±10% [9]. However, the measurement

a. Corresponding author; kilgs@kmou.ac.kr

of reference voltage can not be applied for on-line monitoring as the power must be switched off and the varistor must be disconnected from the circuit.

In this paper, two types of varistors with different specifications were used for the accelerated aging experiment by applying the standard lightning impulse current. The changes in electrical characteristics of varistor with the energy absorption were analyzed. The results from this paper are expected to be applied for on-line condition monitoring of ZnO varistor.

2. METHOD FOR EXPERIMENT

2.1 ZnO Varistors

Two types of ZnO varistors were used and their specifications including maximum continuous operating voltage (MCOV), reference voltage, peak surge current, clamping voltage, maximum energy absorption, and dimension are shown in Table 1. Since the characteristics differ even for the varistors with the same specification, two samples were used for each type of varistor.

Table 1. Specifications of ZnO varistors.

Type	A	B
Model	SVR391D20A	B60K385
MCOV (V_{AC})	250	385
Reference voltage (V)	390	620
Peak surge current (kA)	6.5 @ 8/20 μs	70 @ 8/20 μs
Clamping voltage (V)	650 @ 100 A	1,025 @ 500 A
Max. energy absorption (J)	130	1,200

2.2 Accelerated aging experiment

The varistors equipped in the power supply circuits and surge protective devices may operate frequently or rarely against the surge and overvoltage depending on their operation condition and environment. Therefore, the energized varistors can not be used for accelerated aging experiment. In this paper, the accelerated aging experiment was carried out by applying the 8/20 μs standard impulse current to the varistors with a time interval of 1 minute. The existing researches study the changes in electrical characteristics with the number of surge. However, the magnitudes of impulse current for accelerated aging experiment are different depending on the type of varistor. In addition, the deterioration progress varies with the magnitudes of impulse current. Therefore, this paper studied the changes in electrical characteristics with the surge energy rather than the surge number. Surge energy can be calculated by

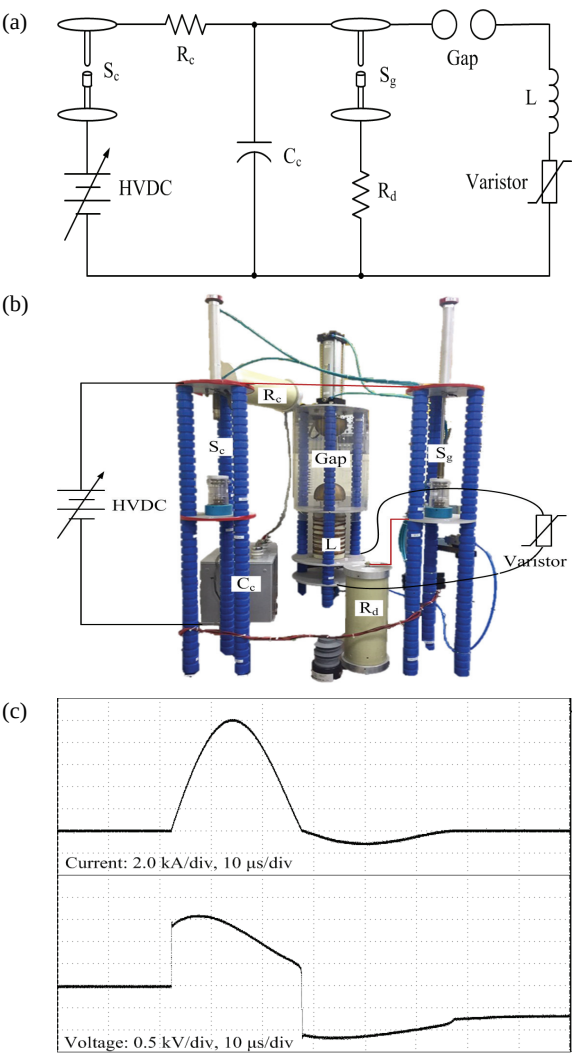

Fig. 1. Configuration of the experimental setup. (a) Equivalent circuit of the impulse current generator, (b) photograph of the impulse current generator, and (c) impulse current and clamping voltage waveforms.

$$W = \int v(t) \cdot i(t)dt \quad (1)$$

where $i(t)$ is the impulse current and $v(t)$ is the clamping voltage of varistor. For varistor SVR391D20A, the magnitude of impulse current was 2 kA and the surge energy was 16 J. The magnitude of impulse current and surge energy for varistor B60K385 were 10 kA and 200 J, respectively.

Figure 1 shows the configuration of experimental setup. The impulse current generator consisted of high voltage direct current (HVDC) module, charging switch S_c, charging resistor R_c, charging capacitor C_c, spark gap, and inductor L. In addition, a grounding switch S_g and a discharge resistor R_d were used for releasing the residual voltage in the charging capacitor. The impulse current was measured using a current transformer (Stangenes, 3-0.01) with an output sensitivity of 0.01 V/A, and the voltage was measured using a high voltage probe (Tektronix, P6015) with a ratio of 1,000 : 1 [10,11]. Figure 1(c) illustrates the waveforms of impulse current and clamming voltage for varistor B60K385. The magnitude of impulse current and clamping voltage were 10 kA and 1.63 kV, respectively.

2.3 Measuring system

Parallel with the accelerated aging experiment, electrical characteristics of varistors in terms of reference voltage (V_{ref}), total leakage current (I_T), resistive leakage current (I_R), and third harmonic component of total leakage current (I_{3rd}) were measured. The reference voltage was defined as the voltage across the varistor at the DC current of 1 mA.

The leakage current measurement is shown in Fig. 2. The total leakage current of the varistor is composed of a capacitive and a resistive component. Therefore, the resistive component can be extracted by subtracting the capacitive leakage current from the total leakage current. In Fig. 2(a), the capacitive and total leakage current were measured through R_1 and R_2, respectively [12]. This circuit is an off-line method but has high accuracy. The signals were acquired using a data acquisition unit (DAQ) with a sampling rate of 100 MS/s and were processed based on LabVIEW program. Figure 2(b) shows the measuring algorithm, which contains parts of signal acquisition, low pass filter (LPF) with a cutoff frequency of 5 kHz, resistive leakage current calculation, third harmonic component extraction based on the fast Fourier transform, and data save. For operating the distinct parts in a programmatically determined dynamic sequence, the standard state machine design pattern was used. Waveforms of total, capacitive, and resistive

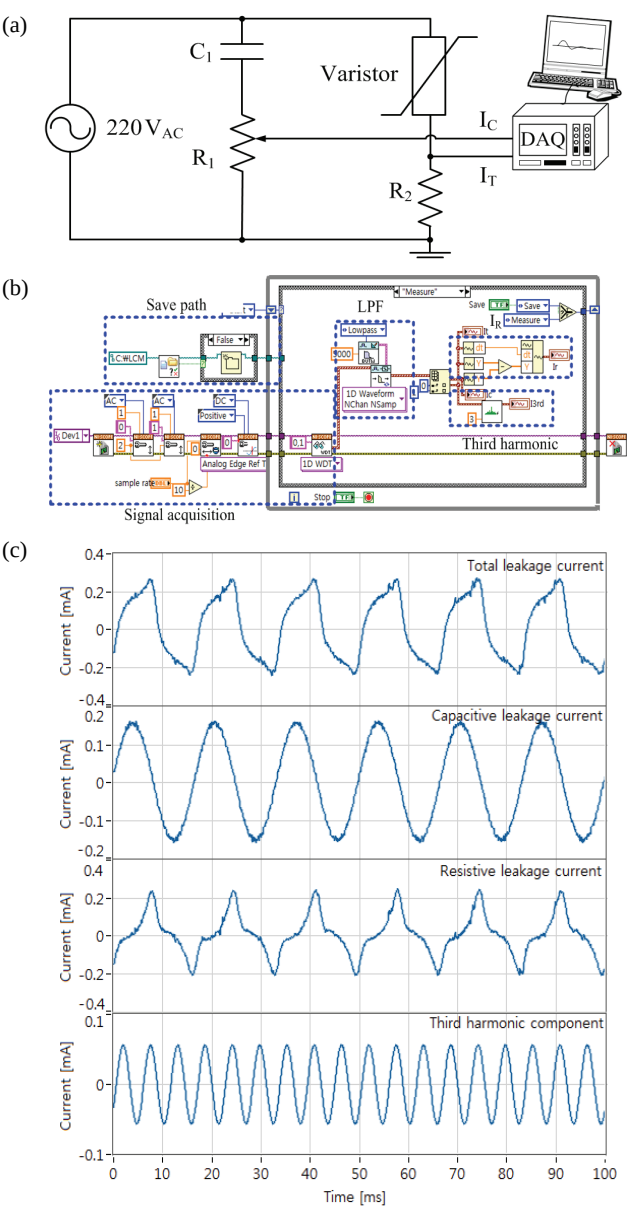

Fig. 2. Leakage current measurement. (a) Circuit diagram, (b) measurement algorithm, and (c) leakage current waveforms of an aged varistor.

leakage current as well as the third harmonic component of total leakage current of an aged varistor are demonstrated in Fig. 2(c).

3. RESULTS AND DISCUSSIONS

For analyzing the changes in electrical characteristics of varistors with the energy absorption, the point where the reference voltage decreased about 10% was taken as a reference. Table 2 shows the initial values of each characteristic and the rates of change are shown in Fig. 3 and Fig. 4.

Table 2. Initial values of electrical characteristics.

Model	SVR391D20A		B60K385	
Sample	A_1	A_2	B_1	B_2
V_{ref} (V)	421	402	624	640
I_T (μA)	101	108	590	595
I_R (μA)	1.47	2.21	1.14	1.22
I_{3rd} (μA)	4.55	6.88	10.1	8.6

The changes in electrical characteristics of varistor SVR391D20A (type A) with the energy absorption are shown in Fig. 3. For sample A_1, the reference voltage decreased by 11% as the varistor absorbed 3.2 kJ surge energy. The total leakage current, resistive leakage current, and third harmonic component of total leakage current increased 1.36, 4.31, and 5.49 times of their initial values, respectively. The total leakage current, resistive leakage current, and third harmonic component of sample A_2 increased 1.45, 3.87, and 5.17 times when the reference voltage decreased by 10%.

Figure 4 shows the changes in electrical characteristics of varistor B60K385 (type B) with the energy absorption. As the volume of ZnO element of B60K385 is much larger than that of SVR391D20A, more surge energy was absorbed by B60K385 for its accelerated aging experiment. When the reference voltage of sample B_1 changed to 0.9

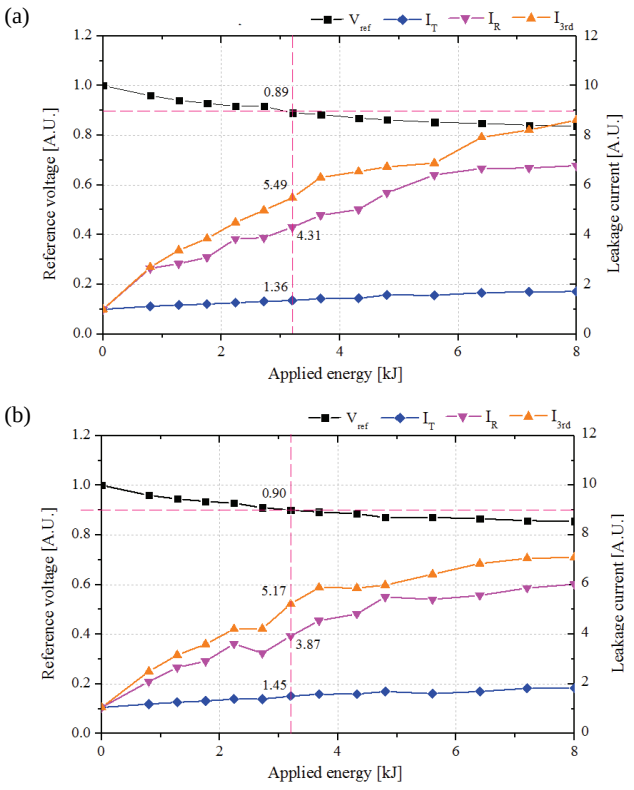

Fig. 3. Changes in electrical characteristics with energy absorption of SVR391D20A. (a) Sample A_1 and (b) sample A_2.

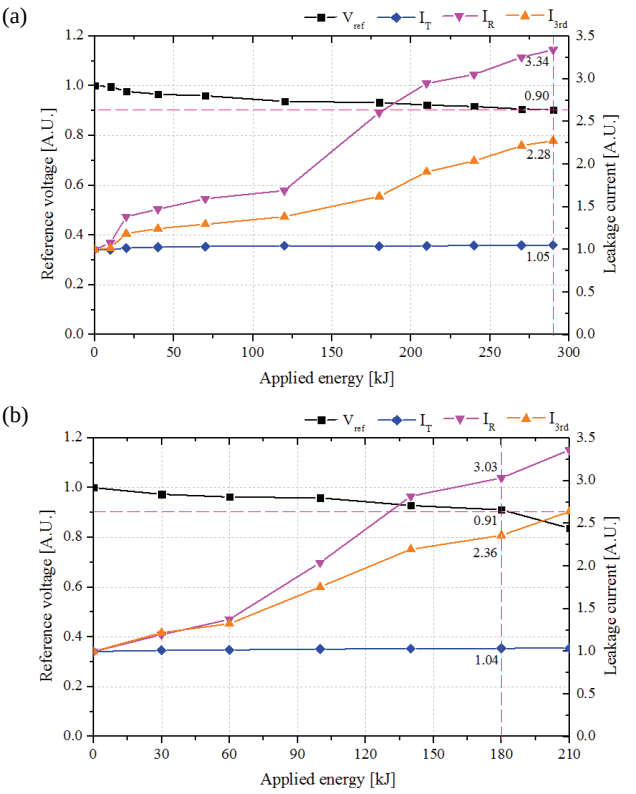

Fig. 4. Changes in electrical characteristics with energy absorption of B60K385. (a) Sample B_1 and (b) sample B_2.

times of its initial value, the total leakage current increased 5%, the resistive leakage current increased 234%, and the third harmonic component increased 128%. For sample B_2, the reference voltage decreased to 0.91 times of its initial value when 180 kJ energy was absorbed. The total leakage current, resistive leakage current, and third harmonic component of total leakage current increased 1.04, 3.03, and 2.36 times comparing with their initial values.

4. CONCLUSION

In this paper, the accelerated aging experiment was conducted to investigate the changes in electrical characteristics of two types of varistors. The impulse current generator was fabricated and the leakage currents were measured by the proposed algorithm. From the results, the following conclusions can be obtained:

1) When the reference voltages of varistors used in this paper decrease by 10%, they are still functional. However, by monitoring the leakage current, especially the resistive leakage current and the third harmonic component, the varistor should be replaced as a further increase in leakage current may cause the thermal runaway.
2) The changes in electrical characteristics have the similar trend even for different types of varistors. The total leakage current increases slightly with the energy absorption, whereas the resistive leakage current and the third harmonic component of total leakage current increase apparently. Therefore, compared with the total leakage current, the resistive leakage current and the third harmonic component are responsible to response the condition of varistor when the reference voltage decreases by 10%.
3) The on-line measurement circuit for resistive leakage current is complicated and its small value results in measuring error, therefore, the third harmonic component of total leakage current is the optimal parameter for on-line condition monitoring of varistor.
4) The changes in electrical characteristics with absorbed energy may vary for varistors with different models due to their rated voltages and specifications. In addition, as a result of difference in manufacturing process, deterioration progresses of the same varistor may be different after absorbing the same energy. However, the third harmonic component can be used for evaluating the condition of a specific varistor. For varistor SVR391D20A and B60K385, the risk levels should be set at 5 and 2 times of the initial values of the third harmonic components, respectively.

REFERENCES

[1] IEC, *IEC 62305-1: Protection Against Lightning - Part 1: General Principles*, 2ed ed. (IEC, Geneva, 2010) p. 60.
[2] IEC, *IEC 62305-4: Protection Against Lightning - Part 4: Electrical and Electronic Systems Within Structures*, 2ed ed. (IEC, Geneva, 2010) p. 12.
[3] IEC, *IEC 61643-11: Low-Voltage Surge Protective Devices - Part 11: Surge Protective Devices Connected to Low-Voltage Power Distribution Systems - Requirements and Test Methods*, 1st ed. (IEC, Geneva, 2011) p. 11.
[4] IEC, *IEC 61643-1: Low-Voltage Protective Devices - Part 1: Surge Protective Devices Connected to Low-Voltage Power Distribution Systems - Requirements and Tests*, 2ed ed. (IEC, Geneva, 2005) p. 81.
[5] C. A. Christodoulou, M. V. Avgerinos, L. Ekonomou, I. F. Gonos, and I. A. Stathopulos, *IET Sci., Meas. Technol.*, **3**, 265 (2009). [DOI: https://doi.org/10.1049/iet-smt:20080123]
[6] H. G. Cho, D. H. You, U. Y. Lee, and H. N. Kim, *J. Korean Inst. Electr. Electron. Mater. Eng.*, **20**, 273 (2007). [DOI: https://doi.org/10.4313/JKEM.2007.20.3.273]
[7] P. Papliński and J. Wańkowicz, *IEEE Trans. Dielectr. Electr. Insul.*, **23**, 3458 (2016). [DOI: https://doi.org/10.1109/TDEI.2016.005873]
[8] J. Lundquist, L. Stenstrom, A. Schei, and B. Hansen, *IEEE Trans. Power Del.*, **5**, 1811 (1990). [DOI: https://doi.org/10.1109/61.103677]
[9] R. B. Standler, *Protection of Electronic Circuits from Overvoltages*, *1st ed.* (John Wiley & Sons, New York, 1989) p. 133.
[10] K. S. Park, G. Wang, S. C. Hwang, S. J. Kim, and G. S. Kil, *J. Korean Inst. Electr. Electron. Mater. Eng.*, **29**, 635 (2016). [DOI: https://doi.org/10.4313/JKEM.2016.29.10.635]
[11] G. Wang, S. J. Kim, S. J. Park, G. S. Kil, and H. K. Ji, *Trans. Electr. Electron. Mater.*, **17**, 289 (2016). [DOI: https://doi.org/10.4313/TEEM.2016.17.5.289]
[12] G. S. Kil, J. S. Han, and M. N. Ju, *Trans. Korean. Inst. Elect. Eng.*, **52**, 42 (2003).